Effect of non-vacuum thermal annealing on high indium content InGaN films deposited by pulsed laser deposition

Tzu-Yu Wang,[1] Sin-Liang Ou,[1] Kun-Ching Shen,[1] and Dong-Sing Wuu[1,2,*]

[1]*Department of Materials Science and Engineering, National Chung Hsing University, Taichung 402, Taiwan*
[2]*Department of Materials Science and Engineering, Da-Yeh University, Changhua 511 Taiwan*
[*]*dsw@nchu.edu.tw*

Abstract: InGaN films with 33% and 60% indium contents were deposited by pulsed laser deposition (PLD) at a low growth temperature of 300 °C. The films were then annealed at 500-800 °C in the non-vacuum furnace for 15 min with an addition of N_2 atmosphere. X-ray diffraction results indicate that the indium contents in these two films were raised to 41% and 63%, respectively, after annealing in furnace. In_2O_3 phase was formed on InGaN surface during the annealing process, which can be clearly observed by the measurements of auger electron spectroscopy, transmission electron microscopy and x-ray photoelectron spectroscopy. Due to the obstruction of indium out-diffusion by forming In_2O_3 on surface, it leads to the efficient increment in indium content of InGaN layer. In addition, the surface roughness was greatly improved by removing In_2O_3 with the etching treatment in HCl solution. Micro-photoluminescence measurement was performed to analyze the emission property of InGaN layer. For the as-grown InGaN with 33% indium content, the emission wavelength was gradually shifted from 552 to 618 nm with increasing the annealing temperature to 800 °C. It reveals the InGaN films have high potential in optoelectronic applications.

OCIS codes: (160.2100) Electro-optical materials; (160.6000) Semiconductor materials.

References and links

1. J. Wu, W. Walukiewicz, K. M. Yu, W. Shan, J. W. Ager, E. E. Haller, H. Lu, W. J. Schaff, W. K. Metzger, and S. Kurtz, "Superior radiation resistance of $In_{1-x}Ga_xN$ alloys: Full-solar-spectrum photovoltaic material system," J. Appl. Phys. **94**(10), 6477–6482 (2003).
2. T. Matsuoka, N. Yoshimoto, T. Sasaki, and A. Katsui, "Wide-gap semiconductor InGaN and InGaAln grown by MOVPE," J. Electron. Mater. **21**(2), 157–163 (1992).
3. S. Keller, S. F. Chichibu, M. S. Minsky, E. Hu, U. K. Mishra, and S. P. DenBaars, "Effect of the growth rate and the barrier doping on the morphology and the properties of InGaN/GaN quantum wells," J. Cryst. Growth **195**(1–4), 258–264 (1998).
4. A. Kobayashi, J. Ohta, and H. Fujioka, "Low temperature epitaxial growth of $In_{0.25}Ga_{0.75}N$ on lattice-matched ZnO by pulsed laser deposition," J. Appl. Phys. **99**(12), 123513 (2006).
5. J. Ohta, H. Fujioka, and M. Oshima, "Room-temperature epitaxial growth of GaN on conductive substrates," Appl. Phys. Lett. **83**(15), 3060–3062 (2003).
6. G. T. Thaler, D. D. Koleske, S. R. Lee, K. H. A. Bogart, and M. H. Crawford, "Thermal stability of thin InGaN films on GaN," J. Cryst. Growth **312**(11), 1817–1822 (2010).
7. H. Hung, K. T. Lam, S. J. Chang, H. Kuan, C. H. Chen, and U. H. Liaw, "Effects of thermal annealing on In-induced metastable defects in InGaN films," Mater. Sci. Semicond. Process. **10**(2–3), 112–116 (2007).
8. P. R. Chalker, D. Morrice, T. B. Joyce, T. C. Q. Noakes, P. Bailey, and L. Considine, "Indium segregation in MOCVD InGaN layers studied by medium energy ion scattering," Diamond Related Materials **9**(3–6), 520–523 (2000).
9. H. W. Seo, L. W. Tu, Y. T. Lin, C. Y. Ho, Q. Y. Chen, L. Yuan, D. P. Norman, and N. J. Ho, "*p*-GaN/InGaN/*n*-GaN pedestal nanorods: Effect of postgrowth annealing on the electrical performance," Appl. Phys. Lett. **94**(20), 201907 (2009).
10. K. C. Shen, T. Y. Wang, D. S. Wuu, and R. H. Horng, "High indium content InGaN films grown by pulsed laser deposition using a dual-compositing target," Opt. Express **20**(14), 15149–15156 (2012).

#183851 - $15.00 USD Received 22 Jan 2013; revised 8 Mar 2013; accepted 10 Mar 2013; published 15 Mar 2013

11. Q. Guo, O. Kato, and A. Yoshida, "Thermal stability of indium nitride single crystal films," J. Appl. Phys. **73**(11), 7969–7971 (1993).
12. K. P. Biju and M. K. Jain, "Annealing studies on InN thin films grown by modified activated reactive evaporation," J. Cryst. Growth **311**(8), 2542–2548 (2009).
13. K. C. Shen, T. Y. Wang, D. S. Wuu, and R. H. Horng, "High thermal stability of high indium content InGaN films grown by pulsed laser deposition," Opt. Express **20**(19), 21173–21180 (2012).
14. A. W. C. Lin, N. R. Armstrong, and T. Kuwana, "X-ray photoelectron/Auger electron spectroscopic studies of tin and indium metal foils and oxides," Anal. Chem. **49**(8), 1228–1235 (1977).
15. H. Parala, A. Devi, F. Hipler, E. Maile, A. Birkner, H. W. Becker, and R. A. Fischer, "Investigations on InN whiskers grown by chemical vapour deposition," J. Cryst. Growth **231**(1–2), 68–74 (2001).
16. D. T. Clark, T. Fok, G. G. Roberts, and R. W. Sykes, "An investigation by electron spectroscopy for chemical analysis of chemical treatments of the (100) surface of n-type InP epitaxial layers for langmuir film deposition," Thin Solid Films **70**(2), 261–283 (1980).
17. V. Y. Davydov, A. A. Klochikhin, V. V. Emtsev, S. V. Ivanov, V. V. Vekshin, F. Bechstedt, J. Furthmuller, H. Harima, A. V. Mudryi, A. Hashimoto, A. Yamamoto, J. Aderhold, J. Graul, and E. E. Haller, "Band Gap of InN and In-Rich $In_xGa_{1-x}N$ alloys ($0.36 < x < 1$)," Phys. Status Solidi, B Basic Res. **230**(2), R4–R6 (2002).

1. Introduction

InGaN alloys with a wide band gap range from 0.7 eV (InN) to 3.4 eV (GaN) are used as the active layers for light emitting diodes (LEDs) to emit blue, green and red lights [1]. In order to grow the InGaN layer with high indium content by metalorganic chemical vapor deposition (MOCVD), the relatively low growth temperature from 500 to 850 °C is required. However, some drawbacks consisting of the low surface mobility of ad-atoms, indium droplets, phase separation, and composition inhomogeneity are always formed during the low-temperature growth process [2, 3]. Recently, the high quality of nitride films were grown by using pulsed laser deposition (PLD) technique at low temperature ranging from 25 to 380 °C [4, 5]. The kinetic energies of atoms were enhanced with the assistance from laser energy, leading to the surface migration of ad-atoms. On the other hand, the treatments of post-annealing at 500-1000 °C have been proposed to estimate the feasibility of InGaN films [6–9]. Chalker *et al.* have demonstrated that the InGaN film with lower indium content was observed after annealing in vacuum due to the loss of indium from surface via inward diffusion and some surface evaporation [8]. However, Seo et al. have found that there was an increase of 2% indium in the InGaN layer after 800 °C-annealing with a N_2 atmosphere in furnace due to the possible formation of InGaN with In-rich phase [9]. Based on the above researches, the InGaN layer with higher indium content could be obtained by combining the PLD technique and post-annealing in the furnace.

In this study, the InGaN layers with two indium contents of 33% and 60% were prepared by PLD using a dual-composition target. After the deposition, the films were post-annealed at 500-800 °C in a non-vacuum furnace to increase the indium content. Moreover, we have investigated the influence of In_2O_3 formation on films surface during annealing process on the characteristics of InGaN.

2. Experimental

InGaN films were deposited on the MOCVD-grown undoped GaN (2 μm) templates using a dual-composition target by PLD. The details of dual-composition target and growth parameter are described in our previous study [10]. The as-deposited InGaN films with indium contents of 33% and 60% were denoted as samples A_0 and B_0, respectively. The films were treated by an isochronal annealing at 500-800 °C in the non-vacuum furnace for 15 min under a N_2 atmosphere, which were denoted as A_{500}-A_{800} and B_{500}-B_{800}, respectively. The crystal orientations of InGaN films were investigated by x-ray diffraction (XRD) and transmission electron microscopy (TEM). The indium contents of InGaN films were estimated by using the Vegard's law, which calculated the InGaN (0002) diffraction peak shift relative to the GaN (0002) peak. The depth profiles of element concentration for the as-deposited and annealed samples were measured by auger electron spectroscopy (AES). The binding state and surface roughness were characterized by x-ray photoelectron spectroscopy (XPS) and atomic force microscopy (AFM), respectively. Room temperature micro-photoluminescence (μ-PL)

#183851 - $15.00 USD Received 22 Jan 2013; revised 8 Mar 2013; accepted 10 Mar 2013; published 15 Mar 2013

measurement was analyzed to investigate the emission characterization by employing a He-Cd laser with 325 nm as an excitation source.

3. Result and discussion

Figures 1(a) and 1(b) show the XRD patterns of A_0-A_{800} and B_0-B_{800}, respectively. As can be seen, a weak InN (0002) peak resulted from the indium vapor directly reacted with the nitrogen plasma was formed in A_0 and B_0. The InGaN (0002) peak position of A_0-A_{800} was shifted from 33.42° to 33.1° (Fig. 1(a)), corresponding to the increment of indium content from 33% to 41%. Meanwhile, the indium content of B_0-B_{600} was raised from 60% to 63% in Fig. 1(b). According to the past research, the InN content would be decomposed to indium and nitrogen as the annealing temperature was higher than 550 °C [11]. All of the A_{600}-A_{800} and B_{600}-B_{800} samples displayed the In_2O_3 peaks, which resulted from the reaction between the indium (produced by the decomposition of InN) and residual oxygen [12]. The AES depth profiles of A_0, B_0, A_{700} and B_{700} were shown in Figs. 1(c)-1(f), respectively. It can be observed that the elements of O, N, In and Ga distributions in A_0 and B_0 were clearly distinguished into the InGaN and GaN regions in Figs. 1(c) and (d), respectively. Figure 1(e) demonstrated that the higher oxygen was distributed on InGaN surface. Furthermore, we also found the oxygen and indium were diffused into the regions of InGaN and GaN. Nevertheless, the serious oxidation and diffusion can be found in Fig. 1(f), resulting from the easy reaction between the higher indium content and incorporation oxygen. This is the reason why the InGaN peaks disappeared in B_{700} and B_{800}, as shown in Fig. 1(b). These results proved that the increase in indium content of InGaN was caused from the In_2O_3 formation on InGaN surface, obstructing the out-diffusion of indium. Therefore, the indium can be reacted with surrounding InGaN toward the higher indium content. In our previous study [13], the InGaN films grown by PLD were then annealed at 500-800 °C in the vacuum chamber with a N_2 atmosphere. It was found that the indium contents of InGaN layers before and after annealing were almost the same, indicating a dissimilar result compared to this study. It is attributed to the In_2O_3 formation on InGaN surface during the non-vacuum annealing process in this study.

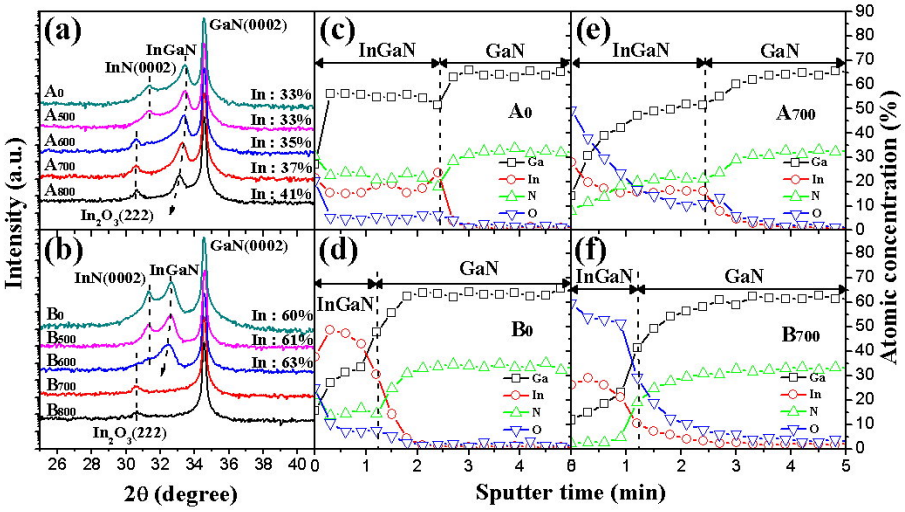

Fig. 1. XRD patterns of samples (a) A_0-A_{800} and (b) B_0-B_{800}. AES depth profile analyses of samples (c) A_0, (d) B_0, (e) A_{700} and (f) B_{700}.

The cross-sectional TEM images of annealed InGaN (A_{600} and B_{600}) were presented in Figs. 2(a) and 2(b), and the thicknesses of these two samples can be determined to 121.8 and 71.9 nm, respectively. Moreover, the oxide thickness of 43.8 nm in B_{600} was higher than that in A_{600} (28.1 nm). It was in good agreement with the AES results, as shown in Figs. 1(b) and

#183851 - $15.00 USD Received 22 Jan 2013; revised 8 Mar 2013; accepted 10 Mar 2013; published 15 Mar 2013

1(f). High resolution images of A_{600} and B_{600} exhibited in Figs. 2(c) and 2(d) were taken at the interface between oxide and InGaN layers, marked with the red-dash line in Figs. 2(a) and 2(b), respectively. From our calculation, the d-spacing of incompletely decomposed InN and crystalline In_2O_3 were 2.85 and 2.92 Å, respectively. The InGaN layer was analyzed to a single crystal structure with (0002) plane. The d-spacing of InGaN (0002) planes in A_{600} and B_{600} were determined to 2.683 and 2.758 Å, which can be indexed to the indium contents of 35% and 63%, respectively. The indium contents in these samples corresponded to the XRD results in Figs. 1(a) and 1(b).

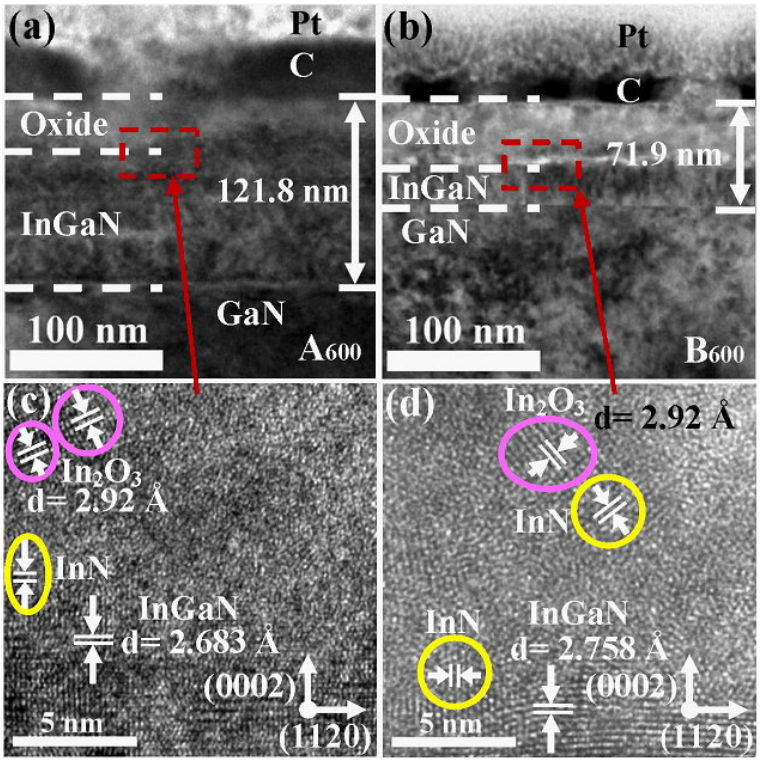

Fig. 2. Cross-sectional TEM images of (a) A_{600} and (b) B_{600}. High resolution images of (c) A_{600} and (d) B_{600} were taken at the interface between InGaN and oxide layers.

Figure 3 shows the XPS spectra of O*1s* and In*3d* for A_0-A_{800} at a sputtering depth of 20 nm. From the spectra of O*1s* binding energy (Fig. 3(a)), there was no In-O peak existed in the samples of A_0 and A_{500}. However, the divided peaks corresponding to 530.5 and 530 eV formed in A_{600}-A_{800} were determined to In_2O_3 phase [14], and the peak intensity was enhanced as the annealing temperature was increased. Moreover, the spectra of In*3d* binding energy were measured to confirm the oxidation states in the films again, as shown in Fig. 3(b). For the spectra of A_0 and A_{500}, almost the same peak positions at 451 and 443.4 eV were analyzed to In$3d_{3/2}$ and In$3d_{5/2}$, respectively, resulting from the In-N bonds [15]. With increasing the annealing temperature to 600-800 °C, the peaks of In$3d_{3/2}$ and In$3d_{5/2}$ were shifted toward higher binding energy and approached to 451.8 and 444.3 eV, respectively. It can be proved the In_2O_3 phase was appeared [16], coinciding with the above results.

As mentioned above, the In_2O_3 was formed during the annealing process (600-800 °C), which probably leaded to the diffusion of In_2O_3 into the InGaN layer. This would cause the existence of In_2O_3 and small amounts of InN:O formation in the InGaN region [12], resulting in the enlargement of InGaN d-spacing and the increase in indium content. To verify if the increment of indium content in InGaN film is partially ascribed to the oxide formation, the samples of A_{500}-A_{800} have been etched in HCl solution. The XRD patterns of A_{500}-A_{800} after

#183851 - $15.00 USD Received 22 Jan 2013; revised 8 Mar 2013; accepted 10 Mar 2013; published 15 Mar 2013

etching in HCl solution for 10 min are shown in Fig. 4(a). Apparently, we found that the In_2O_3 peak was disappeared. Figures 4(b) and 4(c) show the indium contents and root-mean-squared (RMS) roughnesses of A_{500}-A_{800} before and after the etching treatment. It can be seen the indium contents of A_{500} and A_{600} before and after etching were the same. Even though the annealing temperature was further increased, the indium contents of A_{700} and A_{800} were slightly decreased to 36.6% and 40.7%, respectively, compared with the non-etching samples (37% and 41%). In Fig. 4(c), there is an obvious decrease in roughness after etching except for the sample of A_{500}. From our observation, the RMS roughnesses of A_{600}, A_{700} and A_{800} before etching were determined to be 29.5, 31.1 and 95.4 nm, respectively. Meanwhile, the RMS roughnesses of these three samples with removing surface oxide were decreased to 2.67, 5.54 and 9.34 nm, respectively. It demonstrated that the rough surface was induced by oxide formation on InGaN surface.

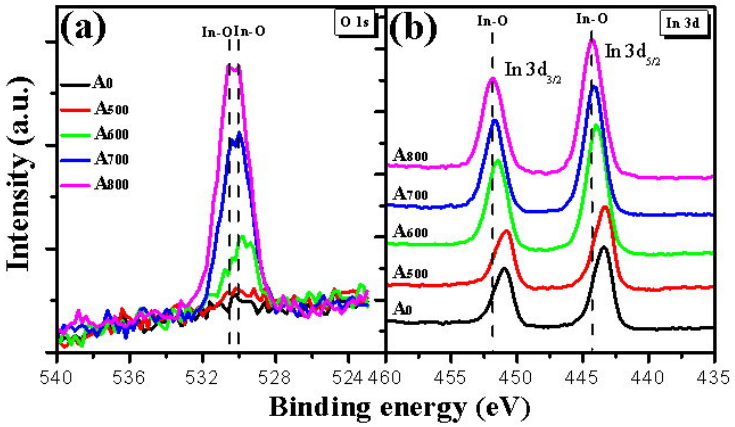

Fig. 3. XPS spectra of (a) O*1s* and (b) In*3d* for the samples of A_0-A_{800} at a sputtering depth of 20 nm.

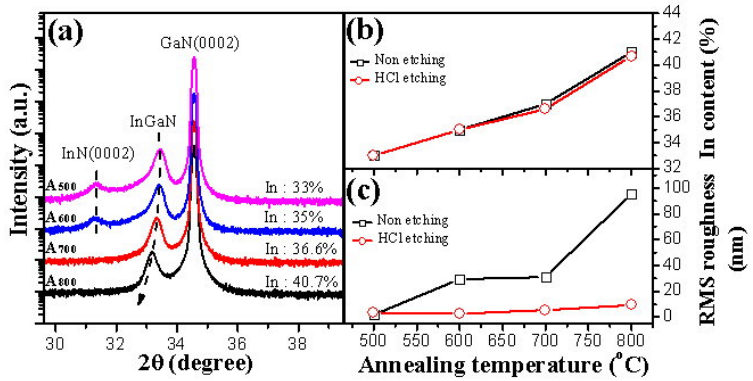

Fig. 4. (a) XRD patterns, (b) Indium contents and (c) RMS roughnesses of A_0-A_{800} before and after etching in HCl solution.

To investigate the luminescent property of InGaN, the μ-PL measurement was performed on the A_0-A_{800} after etching in HCl solution. Figure 5 shows the μ-PL spectra of these samples measured at room temperature. The peak positions of A_0, A_{500}, A_{600}, A_{700} and A_{800} were located at 552, 564, 571, 599 and 618 nm, respectively. It reveals that the emission of InGaN layer was shifted to long wavelength with an increase of annealing temperature. On the other hand, the indium contents of A_0-A_{800} also can be determined from the μ-PL peak positions using the following equation:

#183851 - $15.00 USD Received 22 Jan 2013; revised 8 Mar 2013; accepted 10 Mar 2013; published 15 Mar 2013

$$E(x)=E_{GaN}-x(E_{GaN}-E_{InN})-bx(1-x), \quad (1)$$

where the band gaps of GaN and InN are E_{GaN} = 3.4 eV and E_{InN} = 0.7 eV, respectively. The x and b are represented the indium content and bowing parameter of 1.4 eV, respectively [17]. The indium contents of A_0, A_{500}, A_{600}, A_{700} and A_{800} were estimated as 32%, 33%, 34%, 37% and 39%, respectively. The indium contents determined from μ-PL measurements are very close to those from XRD results shown in Fig. 4(a). Moreover, it proves again that the indium content is increased by raising the annealing temperature.

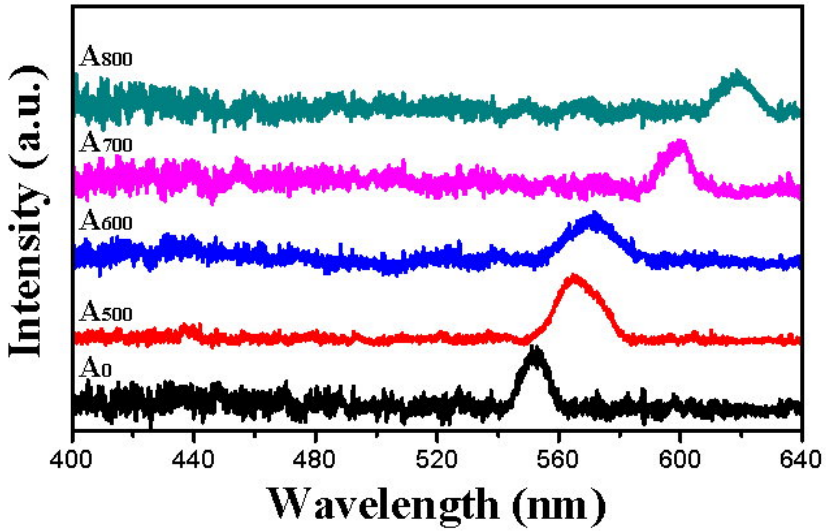

Fig. 5. μ-PL spectra of A_0 and A_{500}-A_{800} etched in HCl solution.

4. Conclusion

InGaN films with indium contents of 33% and 60% were prepared on the MOCVD-grown undoped GaN templates by pulsed laser deposition at 300 °C. Then the films were annealed by using the non-vacuum furnace to investigate the effect of annealing temperature on crystal structure, indium content and emission characterization of InGaN. Because of the In_2O_3 formation on surface during the non-vacuum furnace annealing, it resulted in the blocking of indium out-diffusion from InGaN. Therefore, the indium content of InGaN layer can be increased efficiently. The luminescent property of InGaN measured by micro-photoluminescence indicated the emission peak was shifted to long wavelength with an increment of annealing temperature, corresponding to the trend of increased indium content. This indicates the InGaN films can be potentially useful in optoelectronic devices.

Acknowledgments

This research was supported by National Science Council (Taiwan, R.O.C.) under the Contract Nos.101-3113-E-005-002-CC2 and 101-2221-E-005-023-MY3.

#183851 - $15.00 USD Received 22 Jan 2013; revised 8 Mar 2013; accepted 10 Mar 2013; published 15 Mar 2013